Temperature dependence of the momentum distribution of positronium in MgF_2, SiO_2, and H_2O

Y. Nagai,* M. Kakimoto,† T. Hyodo, and K. Fujiwara‡
Institute of Physics, Graduate School of Arts and Sciences, University of Tokyo, 3-8-1 Komaba, Meguro-ku, Tokyo 153-8902, Japan

H. Ikari
Faculty of Education, Shizuoka University, 836 Otani, Shizuoka 422-8529, Japan

M. Eldrup
Materials Research Department, Riso National Laboratory, DK-4000 Roskilde, Denmark

A. T. Stewart
Department of Physics, Queen's University, Kingston, Ontario, Canada K7L 3N6
(Received 30 November 1999; revised manuscript received 15 February 2000)

Temperature dependence of the momentum distribution of delocalized Bloch-positronium in solids is studied. The momentum distribution of the positronium, which is proportional to the energy integration of the spectral function weighted with the Bose distribution, is expressed in terms of the effective mass and the deformation potential of the crystal for positronium. A simple formula for the shape of the positronium peak in the 1D-ACAR spectrum is derived and applied to the analysis of the experimental data for MgF_2, SiO_2, and H_2O in wide temperature ranges. An extraordinary broadening of the peak shape is observed for MgF_2. It is interpreted as an effect of the umklapp phonon scattering. The diffusion constants of Ps in these materials are also estimated.

I. INTRODUCTION

Positronium (Ps), the bound state of a positron and an electron, forms in various insulators.[1–3] Ps is in a delocalized Bloch-state in some single crystals: quartz, magnesium fluoride, ice, and some alkali halides at low temperatures.[4–7] In such crystals, narrow peaks are observed in the angular correlation of 2γ annihilation radiation (ACAR) spectra, a main peak at the center and satellite peaks at the momenta corresponding to the projections of the reciprocal lattice vectors.[8] These peaks, which originate from the self-annihilation of the Ps, represent the translational momentum distribution of the Ps atoms. The relative intensities of these peaks provide information about the wave function of the Ps.[9,10]

The shape of the central peak enables us to discuss the renormalization and the damping of the Ps state. (We refer to this peak as Ps peak.) The shape $N_{1D}(p_x)$ of the Ps peak in one-dimensional (1D-) ACAR spectra is the linear projection of the Ps momentum distribution. The momentum density distribution $F(\vec{p})$ of the Ps is proportional to the energy integration of the Ps spectral function $\rho_{\vec{p}}(\omega)$ weighted with the Bose distribution:[11]

$$F(\vec{p}) \propto \int_{-\infty}^{\infty} d\omega \frac{\rho_{\vec{p}}(\omega)}{e^{\omega/k_B T}-1}. \tag{1}$$

This shows that the ACAR data reflect the momentum aspect of the spectral function.

In previous works[12,13] investigating the shape of the Ps peak in terms of $F(\vec{p})$, Eq. (1) was approximated for simplicity by a Gaussian function with the same full-width at half-maximum (FWHM). This approach, however, fails for magnesium fluoride where the $N_{1D}(p_x)$ at higher temperatures cannot be approximated by a single Gaussian because of a large tail.[13]

In this paper, we present a formula for the $N_{1D}(p_x)$ expressed in terms of the effective mass of the Ps and the deformation potential without the Gaussian approximation. The linear projection of $F(\vec{p})$ is compared directly with the shape of the Ps peak observed in the 1D-ACAR spectrum. The 1D-ACAR of MgF_2 single crystal is measured in a wide temperature range and the formula is applied to fit the data. The formula is also applied to fit the quartz and ice data which were previously measured. The large tail in the $N_{1D}(p_x)$ for MgF_2 at higher temperatures is well explained by taking into account the effect of the umklapp phonon scattering recently suggested by Bondarev.[14] The diffusion constant is also estimated for each material.

II. THEORY

Since Ps is neutral, its interaction with longitudinal acoustic phonons is expected to be more important than that with polar optical phonons. Our problem is simplified by considering only the interaction with the former as in the theory of the exciton.[15,16] Then the Ps-phonon interaction is treated in terms of the effective mass M^* of the Ps and the deformation potential E_d. The Hamiltonian is written as

$$H = H_0 + H' = \left[\sum_{\vec{k}} \varepsilon_{\vec{k}} c_{\vec{k}}^{\dagger} c_{\vec{k}} + \sum_{\vec{q}} \hbar \omega_{\vec{q}} a_{\vec{q}}^{\dagger} a_{\vec{q}} \right] + \sum_{\vec{k},\vec{q},\vec{G}} g_{\vec{q}} c_{\vec{k}+\vec{q}+\vec{G}}^{\dagger} c_{\vec{k}} (a_{\vec{q}} - a_{-\vec{q}}^{\dagger}), \tag{2}$$

 ©2000 The American Physical Society

$$g_{\vec{q}} = iE_d q \sqrt{\frac{\hbar}{2\omega_q \rho V}}, \quad \varepsilon_{\vec{k}} = \frac{\hbar^2 k^2}{2M^*}, \tag{3}$$

where $a_{\vec{q}}$ annihilates a phonon with frequency $\omega_{\vec{q}}$, $c_{\vec{k}}$ annihilates a positronium atom with kinetic energy $\varepsilon_{\vec{k}}$, ρ is the density of the material, $\vec{G}$ is the reciprocal lattice vector, $g_{\vec{q}}$ is the Ps-phonon coupling constant and V is the volume of the sample. The terms with $\vec{G}=0$ and $\vec{G}\neq 0$ correspond to the normal and umklapp interactions with phonons, respectively. Then the spectral function is well approximated by

$$\rho_{\vec{k}}(\omega) = \frac{2\Gamma_{\vec{k}}(\omega)}{(\omega - \hbar^2 k^2/2M^*)^2 + [\Gamma_{\vec{k}}(\omega)]^2}, \tag{4}$$

with the self-energy $\Sigma_{\vec{k}} = \Delta_{\vec{k}} - i\Gamma_{\vec{k}}$. Substituting Eq. (4) into Eq. (1), we can write the momentum distribution $F(\vec{p})$ of the Ps as

$$F(\vec{p}) \propto \int_0^\infty \frac{\Gamma_{\vec{k}}(\omega) e^{-\omega/k_B T}}{(\omega - p^2/2M^*)^2 + [\Gamma_{\vec{k}}(\omega)]^2} d\omega, \tag{5}$$

where the Bose statistics is replaced by the Boltzmann statistics because there exists at most only one Ps atom at a time in the specimen.

Using the lowest (second) order perturbation theory, the damping term Γ is

$$\Gamma_{\vec{k}}(\omega) \sim \frac{\tilde{E}_d^2 M^{*3/2} k_B T}{\sqrt{2}\pi\hbar^3 s^2 \rho} \sqrt{\omega} \tag{6}$$

with

$$\tilde{E}_d = \sqrt{E_d^2 + \frac{\hbar s^2 E_d^{(1)2} n(\omega_1)}{\omega_1 k_B T}} \approx \begin{cases} E_d & \text{for } T < T_D = \hbar\omega_1/k_B, \\ \sqrt{E_d^2 + (sE_d^{(1)}/\omega_1)^2} & \text{for } T > T_D, \end{cases} \tag{7}$$

where $E_d^{(1)} = E_d \nu G/2$ representing the effect of the umklapp phonon interaction,[14] s is sound velocity, ν is the number of the nearest neighbors in the reciprocal lattice space, $n(\omega_1) = [\exp(\hbar\omega_1/k_B T) - 1]^{-1}$ is the value of the phonon distribution function at the phonon frequency ω_1 near the boundary of the Brillouin zone.

In the previous works,[12,13] the momentum distribution $F(\vec{p})$, derived by substituting Eq. (6) into Eq. (5) without the umklapp effect ($E_d^{(1)}=0$), was approximated by a Gaussian function. However, it is possible to calculate the linear projection of $F(\vec{p})$, i.e., 1D-ACAR spectrum $N_{1D}(p_x)$ for the Ps peaks, without using the Gaussian approximation. The integration over the momenta p_y and p_z can be performed analytically prior to the integration over the energy (ω):

$$N_{1D}(p_x) \propto \int_0^\infty d\xi \xi e^{-\xi^2/k_B T} \left[\frac{\pi}{2} + \arctan\left(\frac{\xi^2 - \gamma p_x^2}{\alpha \xi} \right) \right], \tag{8}$$

$$\alpha = \frac{\tilde{E}_d^2 M^{*3/2} k_B T}{\sqrt{2}\pi\hbar^3 s^2 \rho}, \quad \gamma = \frac{1}{2M^*}. \tag{9}$$

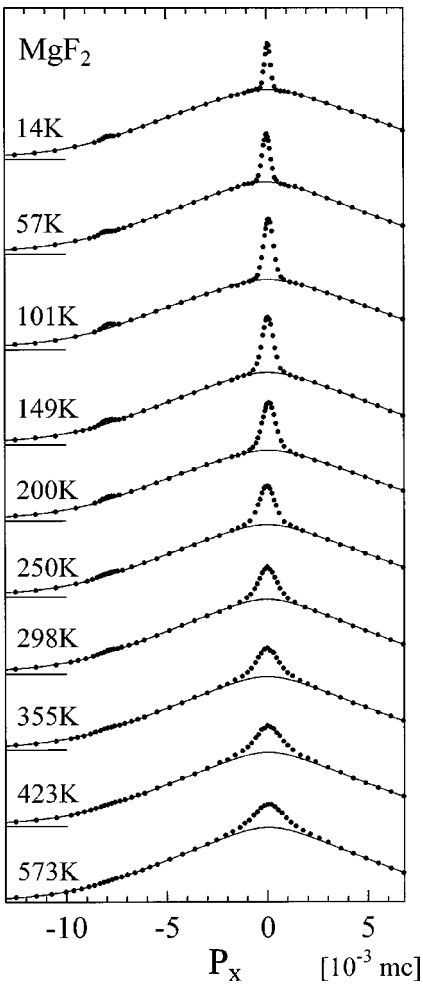

FIG. 1. The angular correlation curves along the c axis of a MgF_2 single crystal taken at temperatures from 14 K to 573 K. The solid lines indicate the broad component irrelevant to the momentum distribution of the Ps.

Since this expression includes only one integration and the two parameters M^* and $\tilde{E}_d$, we can apply nonlinear least squares fit directly to the measured 1D-ACAR data.

III. EXPERIMENTAL

A MgF_2 single crystal cut perpendicular to the c axis was supplied by OKEN Co. Ltd. The 1D-ACAR spectra in a wide temperature range from 14 K to 573 K were measured by using long-slit apparatus. The 1D-projection of the electron-positron momentum distribution to the c axis of the crystal was measured under the magnetic field of 1.5 T. The momentum resolution of the apparatus is well approximated by a Gaussian function with the FWHM of $0.30\times10^{-3}mc$ (m: free electron mass; c: light speed; $mc=137$ a.u.). The reason the c-axis is selected is that the narrow peaks are most widely separated from each other, and hence the subtraction of broad component is the easiest. The obtained data are shown in Fig. 1.

Each ACAR curve consists of a broad component with the FWHM of $\sim 10\times10^{-3}mc$, a narrow strong peak at the center, and a weak satellite peak at the momentum ($-8\times10^{-3}mc$) corresponding to the projection of the (111)

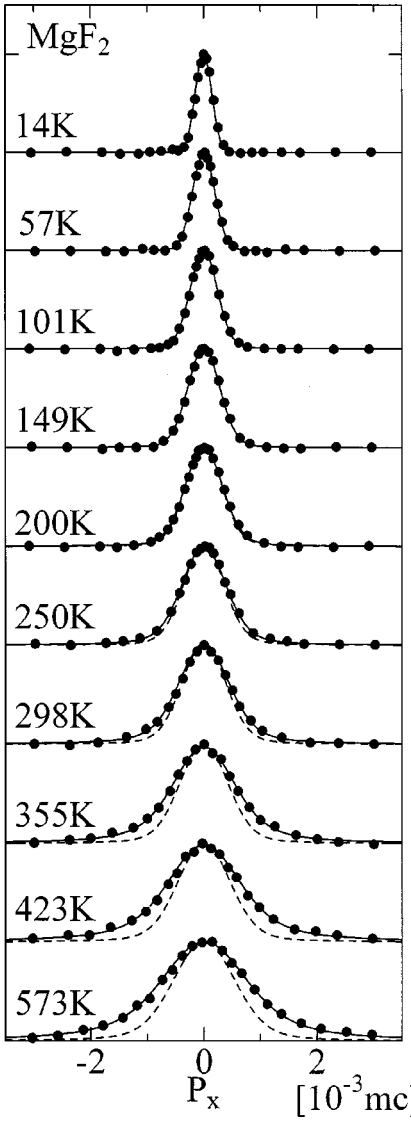

FIG. 2. The central p-Ps peak for MgF_2 at different temperatures. The peaks are extracted by subtracting the broad component from the measured 1D-ACAR curves. The solid and dashed lines are the results of the nonlinear least square fits by Eq. (8).

reciprocal-lattice vector. The narrow peaks are attributed to the 2γ self-annihilation of the delocalized Ps and thus represent the momentum distribution of the Ps. The broad component arises from the annihilation of non-Ps positrons and pick-off annihilation of the Ps (annihilation of the Ps positron with an electron other than that bound in the Ps). This component does not change the shape when the temperature is varied.

The Ps peaks are isolated by subtracting from the 1D-ACAR curves the broad component which is common throughout the whole temperature range. Figure 2 shows the results of the subtraction.

Under the magnetic field, the ortho-Ps can self-annihilate into 2γ due to the Zeemann mixture of the para-Ps and the $m=0$ substate of the ortho-Ps,[17] while 2γ self-annihilation of the ortho-Ps is forbidden in zero field. We have confirmed that the shape of the Ps peak does not depend on the magnetic field. This means that the ortho-Ps, the average lifetime of which is longer than that of para-Ps, is thermalized enough before the annihilation.

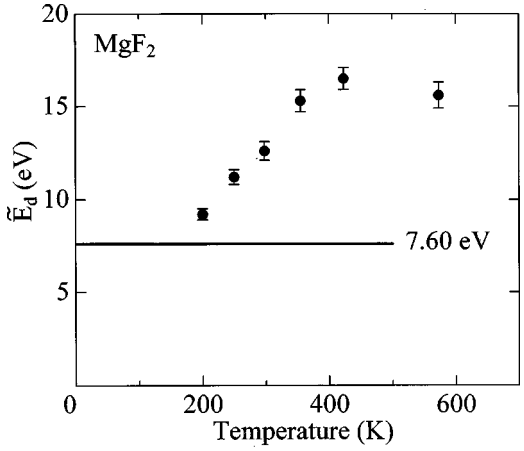

FIG. 3. The temperature dependence of $\tilde{E}_d$ for MgF_2.

IV. ANALYSIS

The formulation described in Sec. II was used to analyze the 1D-ACAR data for the Ps in the MgF_2 crystals. The previously measured data for SiO_2 (α-quartz)[18] and H_2O (ice)[19–21] were also analyzed. The momentum resolutions of the apparatus are well approximated by Gaussian functions with the FWHM of $0.38\times10^{-3}mc$ for the measurements of SiO_2, $0.26\times10^{-3}mc$ for H_2O at 110 K and 160 K, and $0.13\times10^{-3}mc$ for H_2O from 4 K to 60 K. In the case of H_2O, only the data below 160 K were analyzed because a part of the Ps in H_2O is trapped in thermally created vacancies above 180 K and is not in the delocalized Bloch-state.[21] The effect of the momentum resolution of the apparatus is included by convoluting the Gaussian resolution function into Eq. (8) in the fitting procedure.

We tried fitting Eq. (8) to the spectra for MgF_2 with common M^* and $|\tilde{E}_d|$ in the whole temperature range. It was not possible to obtain the common values of the parameters. Then we tried the same fitting in a restricted temperature range, from 14 K to 149 K. The solid lines in Fig. 2 in this temperature range show the results of the fit. The model explains the data very well. The optimized values of $M^*/2m$ and $|\tilde{E}_d|$ are 1.10 ± 0.01 and 7.60 ± 0.09 eV, respectively. Since the T_D of MgF_2 is about 230 K,[22] the $|\tilde{E}_d|$ determined in this temperature range represents $|E_d|$. The sign of E_d is probably negative since both the positron and the electron of the Ps prefer not to penetrate into a molecule and hence Ps likes dilated regions.

The dashed lines above 200 K in Fig. 2 show the Ps peak shape expected from these values of $M^*/2m$ and $|E_d|$. It is clear that the momentum distribution broadens more as the temperature is elevated. We interpret this in terms of the umklapp phonon scattering, fitting Eq. (8) to the spectra above 250 K with adjustable $\tilde{E}_d$ and $M^*/2m$ fixed to 1.10. The solid curves above 250 K in Fig. 2 show the results of the fit and Fig. 3 shows the optimized values of $\tilde{E}_d$. The fits are good. The value of $\tilde{E}_d$ increases with temperature and saturate to about 16 eV above 355 K. This is consistent with

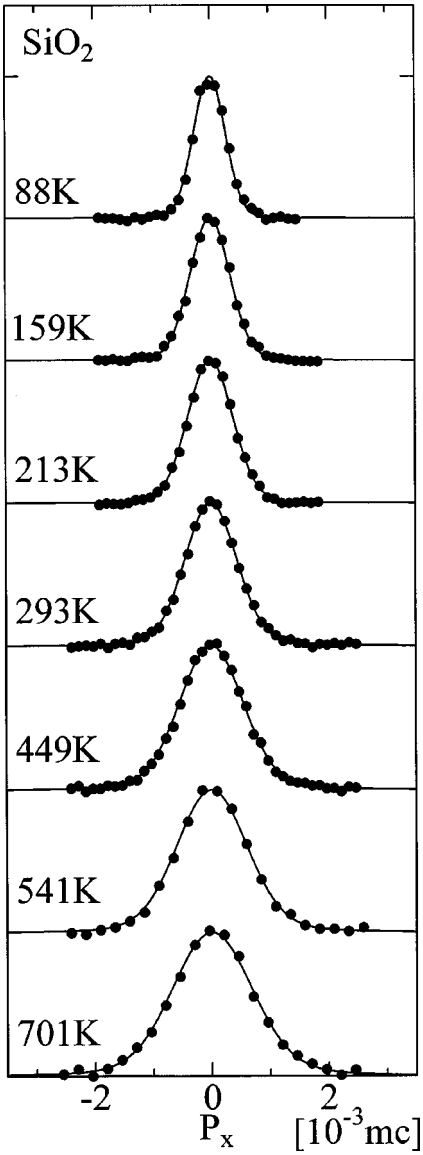

FIG. 4. The central *p*-Ps peak for SiO_2 at different temperatures. The peaks are extracted by subtracting the broad component from the measured 1D-ACAR curves. The solid lines are the results of the nonlinear least square fits by Eq. (8).

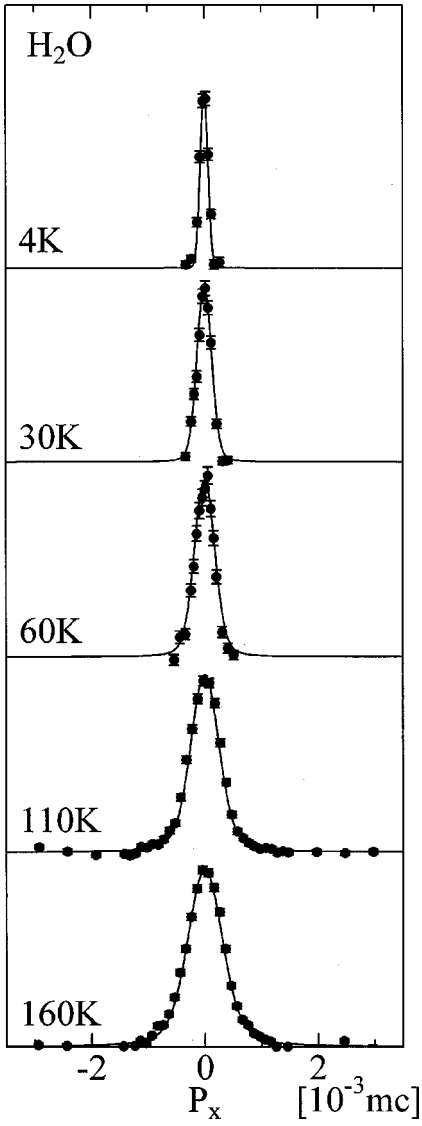

FIG. 5. The central *p*-Ps peak for H_2O at different temperatures. The peaks are extracted by subtracting the broad component from the measured 1D-ACAR curves. The solid lines are the results of the nonlinear least square fits by Eq. (8).

the picture presented by Eq. (7). The value for $E_d^{(1)}$ was obtained to be $\sim 9\times 10^7$ eV/cm, using $\omega_1 = k_B T_D/\hbar$ ($T_D \simeq 230$ K).

Contrary to the case of MgF_2, we can fit, in each the case of SiO_2 and H_2O, Eq. (8) with a common $M^*/2m$ and E_d in the whole temperature range. The results of the fits are shown in Fig. 4 (SiO_2) and Fig. 5 (H_2O). The optimized values are $M^*/2m = 1.54 \pm 0.08$ and $|E_d| = 3.6 \pm 0.7$ eV for SiO_2, and $M^*/2m = 1.1 \pm 0.1$ and $|E_d| = 3.3 \pm 0.6$ eV for H_2O. The fact that one value of E_d can fit all the ice data is in agreement with the Debye temperature being higher than the highest temperature of the measurements.

The diffusion constant D at temperature T is related with Γ and M^* as[2]

$$D \sim \hbar \Gamma_{\vec{k}}^{-1}(k_B T) k_B T / M^*. \tag{10}$$

The obtained values of $M^*/2m$ and $|E_d|$ give the Ps diffsion constant to be $\sim 0.23 \pm 0.06$ cm^2/s for MgF_2 at 300 K, $\sim 0.6 \pm 0.2$ cm^2/s for SiO_2 at 300 K and $\sim 0.3 \pm 0.1$ cm^2/s for H_2O at 100 K.

V. DISCUSSION

With the lowest order approximation of the self-energy, we have been able to explain the 1D-ACAR data for MgF_2, SiO_2, and H_2O very well in terms of the only two parameters, M^* and $|\tilde{E}_d|$. Anomalous broadening for MgF_2 is interpreted as the effect of the umklapp phonon scattering. The other possibility is Ps scattering with the nonpolar optical phonons because the interaction matrix element has the same q-dependence as the umklapp scattering with acoustic phonons. The anormalous broadening is not observed in SiO_2 or H_2O. The reason is not clear at present. Probably $E_d^{(1)}$ for SiO_2 or H_2O is much smaller than that in MgF_2. Even if it is not small in H_2O, we should not expect to see

the effect since the T_D [$\sim$220 K Ref. 23] of H_2O is higher than the highest temperature of the measurements.

The diffusion constants of the Ps in SiO_2 and H_2O have been estimated by using slow positron beams.[24,25] Eldrup *et al.*[24] measured the incident positron energy dependence of the fraction of the Ps emitted from the H_2O surface. The values of D estimated for two different samples were 0.11 and 0.30 cm^2/s below 100 K, which are similar to the present value. Sferlazzo *et al.*[25] estimated the value of D for SiO_2 at room temperature as 0.07 cm^2/s with a method similar to that of Ref. 24. This is one order of magnitude smaller than the present value. The discrepancy could be due to the differences in impurity and defect densities in the sample used, giving rise to differences in Ps scattering and trapping and influencing the effective Ps diffusion constant.

It is to be pointed out that the successful fit of our expression to the data for H_2O shown in Fig. 5 suggests a $T^{-1/2}$ behavior of D as indicated by Eq. (6) inserted into Eq. (10), while a variable-energy positron experiment[24] reports that the D for H_2O is constant below 100 K. It would be interesting to do new and more detailed slow positron experiments on H_2O.

ACKNOWLEDGMENTS

We would like to thank Dr. I. V. Bondarev for useful discussions. This work was supported by a Grant-in-Aid for scientific research (No. 08404018 and No. 7-3800) from the Ministry of Education, Science and Culture of Japan.

*Present address: The Oarai Branch, Institute for Materials Research, Tohoku University, Oarai, Ibaraki 311-1313, Japan.

†Present address: Communication & Information System Laboratories, R & D Center, Toshiba, 1 Komukai, Toshiba-Cho, Kawasaki, Kanagawa 212-8582, Japan

‡Deceased.

[1] K. Fujiwara, in *Positron Annihilation*, edited by P. G. Coleman, S. C. Sharma, and L. M. Diana (North-Holland, Amsterdam, 1982), p. 615.

[2] M. Dupasquier, in *Positron Solid State Physics*, edited by W. Brandt and A. Dupasquier (North-Holland, Amsterdam, 1983) p. 510.

[3] T. Hyodo, in *Positron Annihilation*, edited by P. C. Jain, R. M. Singru, and K. P. Gopinathan (World Scientific, Singapore, 1985), p. 643.

[4] W. Brandt, G. Coussot, and R. Paulin, Phys. Rev. Lett. **23**, 522 (1969).

[5] O. Mogensen, G. Kvajic, M. Eldrup, and M. Milosevic-Kvajic, Phys. Rev. B **4**, 71 (1971).

[6] G. Coussot, Ph.D. thesis, University of Paris, 1970.

[7] J. Kasai, T. Hyodo, and K. Fujiwara, J. Phys. Soc. Jpn. **57**, 329 (1988), and references therein.

[8] A. Greenberger, A. P. Mills, A. Thompson, and S. Berko, Phys. Lett. **32A**, 72 (1970).

[9] C. H. Hodges, B. T. A. McKee, W. Triftshauser, and A. T. Stewart, Can. J. Phys. **50**, 103 (1972).

[10] Y. Nagai, H. Saito, Y. Nagashima, N. Kobayashi, and T. Hyodo, J. Phys.: Condens. Matter **9**, 11 239 (1997).

[11] P. C. Martin and J. Schwinger, Phys. Rev. **115**, 1342 (1959).

[12] H. Ikari, J. Phys. Soc. Jpn. **46**, 97 (1979).

[13] M. Kakimoto, T. Hyodo, and K. Fujiwara, in *Positron Annihilation*, edited by P. C. Jain, R. M. Singru, and K. P. Gopinathan (Ref. 3), p. 776.

[14] I. V. Bondarev, Pis'ma Zh. Éksp. Teor. Fiz. **69**, 215 (1999) [JETP Lett. **69**, 231 (1999)].

[15] Y. Toyozawa, Prog. Theor. Phys. **20**, 53 (1953).

[16] Y. Toyozawa, Prog. Theor. Phys. Suppl. **12**, 111 (1959).

[17] See, for example, A. Rich, Rev. Mod. Phys. **53**, 127 (1981).

[18] H. Ikari and K. Fujiwara, J. Phys. Soc. Jpn. **46**, 92 (1979).

[19] R. J. Douglas, M. Eldrup, L. Lupton, and A. T. Stewart, in *Positron Annihilation*, edited by R. R. Hasiguti and K. Fujiwara (Japan Institute of Metals, Sendai, Japan, 1979), p. 621.

[20] M. Eldrup, in *Positron Annihilation*, edited by P. G. Coleman, S. C. Sharma, and L. M. Diana (Ref. 1), p. 753.

[21] O. E. Mogensen and M. Eldrup, Riso Rep., **366** (1977).

[22] *Phonon Dispersion Relations in Insulators*, edited by H. Bilz and W. Kress (Springer, Berlin, 1979).

[23] F. H. Fletcher, *The Chemical Physics of Ice* (Cambridge University Press, Cambridge, England, 1970), p. 143.

[24] M. Eldrup, A. Vehanen, P. J. Schultz, and K. G. Lynn, Phys. Rev. B **32**, 7048 (1985).

[25] P. Sferlazzo, S. Berko, and K. F. Canter, Phys. Rev. B **35**, 5315 (1987).